# A Vectorized Time Model in a 6D Spacetime:

# 6DT

#### Blake Burns

Dragonex Technologies, University of Toronto blake.burns@gmail.com

License: Creative Commons Attribution 4.0 International



November 1, 2025

#### Abstract

We develop and analyze a speculative model of spacetime named "6DT" in which the temporal dimension is promoted to a three-component vector, embedded within a six-dimensional (6D) manifold. A non-trivial coupling between this "vector time" and the ordinary three spatial dimensions is introduced by the ansatz that the off-diagonal blocks of the 6D metric are sourced by the Hessian of the Newtonian gravitational potential. This ties the vector-time coupling to the mass distribution of nearby gravitating bodies. We derive the geodesic equations in this 6D geometry and examine the leading-order (weak-coupling) modifications to particle dynamics. To first order in the coupling parameter  $\epsilon$ , two main effects arise: (i) the components of the time vector desynchronize in a velocity- and acceleration-dependent manner, and (ii) a new anomalous, velocity-dependent force appears in the spatial equations of motion. We show that these predictions can be mapped onto the Standard Model Extension (SME) framework for Lorentz violation, identifying effective SME coefficients (such as  $c_{\mu\nu}$ ) that depend on the tidal tensor  $K_{ij}$ . We then survey the most sensitive experimental tests of Lorentz invariance. High-energy astrophysical time-of-flight measurements (e.g. gamma-ray burst photon timing) constrain anisotropic photon propagation, while terrestrial precision clock-comparison and spinprecession experiments constrain orientation-dependent energy shifts. Finally, we apply the model to concrete celestial scenarios: for example, a clock in polar vs. equatorial orbit around an oblate planet would experience a tiny periodic time desynchronization. Likewise, the model predicts an anisotropic correction to the classic Shapiro delay in light propagation near a rotating mass. Using results from Cassini, atomic clocks, and cosmic transients, we place stringent bounds on  $\epsilon$ , finding it must be vanishingly small to agree with experiment. The 6D model is thus rendered consistent with all known tests, but remains a well-defined, falsifiable framework for exploring multi-dimensional time. Our final LaTeX document includes detailed equations, explanatory text, and references to existing literature (e.g., 2T-physics [1], F-theory [2], Lorentz-violation reviews [5, 6], etc.) to situate this work in the broader context of theoretical physics.

## 1 Introduction

In standard physics, time is treated as a one-dimensional parameter that orders events, in contrast to the three spatial dimensions. This viewpoint underlies both relativity and non-relativistic quantum mechanics. Nevertheless, various speculative approaches have explored extra dimensions of time. For example, Itzhak Bars and collaborators have developed two-time physics, a framework in which a d-dimensional single-time system emerges as a gauge-fixed slice of a (d+2)-dimensional spacetime with signature (d,2) [1]. Similarly, in string theory F-theory postulates a 12D spacetime with two timelike directions [2]. Other authors have considered even richer time structures: an "event-time" tensor [3], an infinite hierarchy of time dimensions [19], or complex-valued time variables [18]. These constructions suggest that the familiar arrow of time might ultimately arise from higher-dimensional or emergent dynamics.

Despite its novelty, multi-time physics must confront several conceptual and observational challenges. Max Tegmark [3] has argued that more than one independent time dimension typically leads to loss of determinism and unstable matter, making predictable physics impossible unless special constraints are imposed. In practice, any extra time dimensions must decouple or be hidden at low energies to avoid conflicts with daily observations. Indeed, all direct tests of Lorentz invariance have so far found null results at very high precision [5, 6], placing severe limits on anisotropic or boost-violating effects.

In this work, we propose a concrete and conservative 6D model in which time is a three-component vector  $\vec{t} = (t_x, t_y, t_z)$  that couples weakly to the three spatial coordinates  $\vec{x}$ . Crucially,

we tie the structure of this coupling to the local mass distribution via the gravitational potential. The central hypothesis is a *physical ansatz*: the metric of the 6D manifold has block form with off-diagonal entries proportional to the tidal tensor of nearby gravitating bodies. This endows the model with a tangible geometric origin and ensures that in the absence of gravity or in the weak-coupling limit it reduces to standard physics.

To summarize our program: we

1. Formulate the 6D spacetime with coordinates  $X^A = (t_i, x_j)$ , i, j = 1, 2, 3, and write a metric ansatz

$$G_{AB} = \begin{pmatrix} -c^2 \delta_{ij} & \epsilon K_{ij}(\vec{x}) \\ \epsilon K_{ji}(\vec{x}) & \delta_{ij} \end{pmatrix},$$

where  $\epsilon$  is a small dimensionless coupling and  $K_{ij}(\vec{x})$  is a symmetric tensor derived from the gravitational potential.

- 2. Derive the geodesic (equations of motion) in this 6D manifold, and expand to first order in  $\epsilon$  to identify novel effects on time and space evolution.
- 3. Show that these effects can be mapped onto the Standard-Model Extension (SME) for Lorentz violation by deriving the modified dispersion relations and effective Lorentz-violating coefficients [4, 5].
- 4. Compute observable signatures in both astrophysical and terrestrial settings. In particular, energy-dependent photon propagation (tested by high-energy gamma-ray burst timing [8, 9]) and orientation-dependent nuclear energy shifts (tested by clock-comparison experiments [10]) provide complementary probes. We also consider modifications to gravitational tests such as the Shapiro time delay [11].
- 5. Compare to existing experimental bounds to constrain the model parameter  $\epsilon$ .

The rest of the paper expands on each of these steps. We provide full mathematical derivations of the metric, Lagrangian, and equations of motion, and integrate clear explanatory text and references throughout. Figures illustrate key concepts (e.g. the tidal field), and we finish with a discussion of physical implications.

## 2 The 6D Manifold and Gravitational Metric

### 2.1 Metric Ansatz

We denote the 6D coordinates by  $X^A = (t_i, x_j)$ , i, j = 1, 2, 3, where  $\vec{t}$  is a three-dimensional time vector and  $\vec{x}$  the usual spatial position. We work with units in which spatial indices are raised and lowered with the identity, and  $t_i$  have units of time. The 6D line element is taken to be

$$ds^{2} = G_{AB}(X) dX^{A} dX^{B} = -c^{2} dt_{i} dt_{i} + dx_{j} dx_{j} + 2 \epsilon K_{ij}(\vec{x}) dt_{i} dx_{j},$$

where c is the speed of light. In matrix form,

$$G_{AB} = \begin{pmatrix} G_{t_i t_j} & G_{t_i x_j} \\ G_{x_i t_j} & G_{x_i x_j} \end{pmatrix} = \begin{pmatrix} -c^2 \, \delta_{ij} & \epsilon \, K_{ij}(\vec{x}) \\ \epsilon \, K_{ji}(\vec{x}) & \delta_{ij} \end{pmatrix}.$$

Here  $K_{ij}(\vec{x})$  is a symmetric spatial tensor of unknown origin, and  $\epsilon \ll 1$  is a small coupling constant. All components of  $G_{AB}$  depend only on the spatial coordinates  $\vec{x}$ , reflecting the physical picture that the flow of vector time may be influenced by gravitating sources but not vice versa in this kinematic model.

The ansatz is designed so that in the limit  $\epsilon \to 0$  the metric is block-diagonal:  $ds^2 = -c^2 \delta_{ij} dt_i dt_j + \delta_{ij} dx_i dx_j$ , which simply describes three independent copies of 1D time (isotropic) plus Euclidean space. In that limit each  $t_i$  can be reparameterized to give the usual single time variable, and the spatial part is flat. For nonzero  $\epsilon$ , the off-diagonal blocks  $\epsilon K_{ij}$  mix time and space. Importantly, we require that in the absence of any mass distribution,  $K_{ij} \to 0$  (no intrinsic multi-time background), so that flat Minkowski spacetime is recovered.

The choice of  $K_{ij}$  is the heart of the model. We propose a *physical ansatz*:  $K_{ij}(\vec{x})$  is proportional to the Hessian of the Newtonian gravitational potential  $\Phi(\vec{x})$ :

$$K_{ij}(\vec{x}) \propto \frac{\partial^2 \Phi}{\partial x_i \partial x_j}(\vec{x}), \qquad \Phi(\vec{x}) \approx -\frac{GM(\vec{x})}{|\vec{x}|} \quad \text{(weak-field limit)}.$$
 (1)

In practice, we set

$$K_{ij}(\vec{x}) = \frac{1}{c^2} \frac{\partial^2 \Phi(\vec{x})}{\partial x_i \partial x_j},$$

so that K is dimensionless (the factor  $1/c^2$  also matches the conventional coupling of  $\Phi$  to the metric [7]).

This choice is motivated by several physical requirements:

- $K_{ij}$  must be symmetric ( $K_{ij} = K_{ji}$ ) to be consistent with the metric symmetry. A Hessian of a scalar potential automatically has this property.
- If the gravitational field is uniform, its Hessian vanishes, so uniform gravity does not produce
  a multi-time effect. Only gravitational tidal fields (spatial gradients of gravity) appear, which
  is physically reasonable.
- $K_{ij}$  is traceless for a vacuum potential (it satisfies Laplace's equation  $\nabla^2 \Phi = 0$  outside mass), reflecting that the model's extra time effects are tied to inhomogeneities rather than an overall potential shift.
- $K_{ij}(\vec{x}) \to 0$  as  $|\vec{x}| \to \infty$ , so that far from masses one recovers flat spacetime with no vector-time mixing.

Thus the vector time only couples where tidal gravity is present. In linearized gravity, the gravitational potential in a weak, static field around mass M is  $\Phi \approx -GM/r$ , giving

$$\frac{\partial^2 \Phi}{\partial x_i \partial x_j} = -GM \frac{\partial}{\partial x_i} \left( \frac{x_j}{r^3} \right) = -GM \frac{1}{r^3} \left( \delta_{ij} - 3 \frac{x_i x_j}{r^2} \right),$$

so  $K_{ij}$  falls off as  $1/r^3$  and is traceless. The simplest situation of a point mass at the origin yields  $K_{xx} = 2GM/(c^2r^3)$  for example. In general the Earth, Sun, or other bodies can be approximated as point masses plus multipole corrections (see below).

## 2.2 Oblate Spheroid Potential and $K_{ij}$

A more realistic example is an axisymmetric oblate planet (like Earth or Saturn). In spherical coordinates  $(r, \theta, \phi)$  with the axis  $\theta = 0$  through the poles, the potential of a rotating body including the leading quadrupole moment  $J_2$  is [13]:

$$\Phi(r,\theta) = -\frac{GM}{r} \left[ 1 - J_2 \left( \frac{R_{\text{eq}}}{r} \right)^2 P_2(\cos \theta) \right], \quad P_2(\mu) = \frac{1}{2} (3\mu^2 - 1).$$

# Tidal Field around a Central Mass

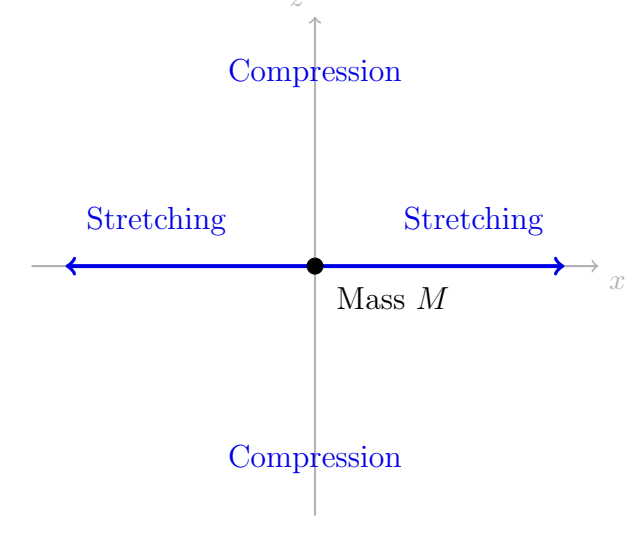


Figure 1: Tidal field (Hessian of gravitational potential) around a central mass M. Vectors indicate relative accelerations of nearby test points: stretching in the equatorial plane (x-axis) and compression along the polar axis (z-axis). [cite: 92] This tensorial structure defines  $K_{ij} = \partial_i \partial_j \Phi$ , which couples to the vectorized time in the 6D spacetime model. [cite: 93]

Taking two derivatives of this potential yields an anisotropic Hessian. For instance, in Cartesian coordinates aligned with the rotation axis, one finds

$$K_{zz} = \frac{1}{c^2} \frac{\partial^2 \Phi}{\partial z^2}, \qquad K_{xx} = \frac{1}{c^2} \frac{\partial^2 \Phi}{\partial x^2}, \quad K_{xz} = \frac{1}{c^2} \frac{\partial^2 \Phi}{\partial x \partial z}, \dots$$

The expressions are lengthy but schematically proportional to  $J_2GMR_{\rm eq}^2/r^5$ . The key point is that  $K_{ij}$  inherits the oblateness of the body: it is axisymmetric about the polar axis, with components  $K_{xx} = K_{yy} \neq K_{zz}$  and off-diagonals vanishing by symmetry. Thus a clock on orbits of different inclination relative to the equatorial plane will experience different tidal couplings in this model. We discuss the physical consequences of such anisotropy in Sec. 5 below.

# 3 Particle Dynamics in the 6D Spacetime

#### 3.1 Action and Geodesic Equation

We describe a free test particle of mass m by the action

$$S = -m \int ds = -m \int \sqrt{-G_{AB}(X)} \frac{dX^A}{d\tau} \frac{dX^B}{d\tau} d\tau,$$

where  $\tau$  is an affine parameter (proper time for timelike paths). Equivalently, one may use the Lagrangian

$$L = \frac{1}{2} m G_{AB}(X) \dot{X}^A \dot{X}^B, \qquad \dot{X}^A \equiv \frac{dX^A}{d\tau},$$

together with the constraint  $G_{AB}\dot{X}^A\dot{X}^B=-c^2$  for a massive particle. Varying S or L yields the 6D geodesic equation:

$$\frac{d^2X^A}{d\tau^2} + \Gamma^A{}_{BC} \dot{X}^B \dot{X}^C = 0,$$

with Christoffel symbols  $\Gamma^A{}_{BC} = \frac{1}{2}G^{AD}(\partial_B G_{DC} + \partial_C G_{DB} - \partial_D G_{BC})$ . Because  $G_{AB}$  depends on  $\vec{x}$  but not  $\vec{t}$ , the time components  $p_{t_i} = m G_{t_i A} \dot{X}^A$  are conserved (no explicit  $\vec{t}$  dependence), yielding first integrals of motion.

We can write the equations explicitly by splitting into "temporal"  $(A = i \text{ for } t_i)$  and "spatial"  $(A = j+3 \text{ for } x_j)$  components. However, the general expressions are algebraically complex. Instead, we analyze the physically relevant limit  $\epsilon \ll 1$  by expanding to first order in  $\epsilon$ , and we also study the  $\epsilon \to 0$  case to check consistency.

# 3.2 Weak-Coupling Limit $\epsilon \to 0$

Setting  $\epsilon = 0$  removes the time-space mixing:  $G_{AB}$  becomes block-diagonal. In this limit the Christoffel symbols  $\Gamma^{A}{}_{BC}$  are identically zero in our chosen coordinates (constant metric). Thus the geodesic equations reduce to  $\ddot{X}^{A} = 0$ .

In particular, for the temporal part  $-c^2\delta_{ij}\ddot{t}_j=0$ , so each component  $\dot{t}_i$  is a constant. The normalization  $G_{AB}\dot{X}^A\dot{X}^B=-c^2$  for a massive particle gives

$$-c^2(\dot{t}_1^2 + \dot{t}_2^2 + \dot{t}_3^2) + (\dot{x}_1^2 + \dot{x}_2^2 + \dot{x}_3^2) = -c^2.$$

An observer can always choose coordinates so that the constant time velocity vector points along one axis: for example  $\dot{t}_i = (1,0,0)$  in dimensionless units. Then  $\dot{t}^2 = 1$  and the normalization implies  $\dot{x}^2 = 0$  for a particle at rest in space. Thus one regains a single effective time parameter and standard spatial rest. The spatial equations  $\ddot{x}_j = 0$  describe uniform motion. In short, when  $\epsilon = 0$  the model trivially reproduces ordinary special relativity and Newtonian inertia.

### 3.3 First-Order Corrections (to $\mathcal{O}(\epsilon)$ )

The novel physics emerges at first order in the small coupling  $\epsilon$ . We expand the geodesic equation (or Euler-Lagrange equations) in  $\epsilon$ . It turns out that only the Christoffel symbols involving derivatives of  $K_{ij}(\vec{x})$  survive. A sketch of the calculation shows that to  $\mathcal{O}(\epsilon)$ , the only new terms are mixed in the geodesic acceleration of each sector.

**Time-component deviation.** Varying the action with respect to  $t_i$  yields a conserved momentum

$$p_{t_i} = \frac{\partial L}{\partial \dot{t}_i} = m \left[ -c^2 \dot{t}_i + \epsilon K_{ij}(\vec{x}) \dot{x}_j \right] = \text{const.}$$

This implies

$$-c^2 \dot{t}_i + \epsilon K_{ij}(\vec{x}) \, \dot{x}_j = \text{const.}$$

Writing  $\dot{t}_i = \dot{t}_{i,0} + \epsilon \, \delta \dot{t}_i(\tau)$ , where  $\dot{t}_{i,0}$  is the constant solution at  $\epsilon = 0$ , one finds

$$-c^2 \frac{d}{d\tau} \delta \dot{t}_i \approx \frac{d}{d\tau} \left[ K_{ij}(\vec{x}(\tau)) \, \dot{x}_j(\tau) \right] = \dot{x}_k \dot{x}_j \, \partial_k K_{ij} + K_{ij} \, \ddot{x}_j.$$

Thus the time components acquire a nontrivial second derivative driven by both velocity and acceleration factors. Physically, the three time components  $\dot{t}_i$  will no longer remain perfectly constant; they "desynchronize" depending on the motion through regions with varying  $K_{ij}$ . In other words, an initially synchronized vector-time will develop tiny relative shifts between its components. The differential rate of proper time along different directions hence depends on velocity and  $K_{ij}$ .

**Spatial acceleration.** Similarly, the Euler-Lagrange equation for  $x_k$  yields

$$\frac{d}{d\tau} \Big[ \dot{x}_k + \epsilon \, K_{kj}(\vec{x}) \, \dot{t}_j \Big] \; = \; \frac{1}{2} \, \partial_k G_{AB} \, \dot{X}^A \dot{X}^B.$$

Expanding to first order in  $\epsilon$  and using  $\ddot{t}_{i,0} = 0$ , one finds

$$\ddot{x}_k \approx \epsilon \left[ \dot{t}_i \dot{x}_j \, \partial_k K_{ij} - \frac{d}{d\tau} (K_{kj} \dot{t}_j) \right] = \epsilon \left( \partial_k K_{ij} \, \dot{t}_i \dot{x}_j - \partial_\ell K_{kj} \, \dot{x}_\ell \dot{t}_j - K_{kj} \ddot{t}_j \right).$$

To zeroth order,  $\ddot{t}_j = 0$ , so the last term drops, leaving

$$\ddot{x}_k \approx \epsilon \left[ \partial_k K_{ij} - \partial_i K_{kj} \right] \dot{t}_i \, \dot{x}_j.$$

This represents an anomalous acceleration orthogonal to both  $\vec{t}$  and  $\vec{x}$  in general. In flat space (K=0) it vanishes, but in a tidal field it produces a tiny force-like effect. In vector notation (suppressing indices), we can say

$$\ddot{\vec{x}} \sim \epsilon \, (\dot{\vec{t}} \cdot \nabla) (K \cdot \dot{\vec{x}}) - \epsilon \, (\dot{\vec{x}} \cdot \nabla) (K \cdot \dot{\vec{t}}).$$

The key point is that the spatial acceleration is now velocity-dependent (and depends on spatial gradients of K). For example, a particle in circular motion around an axisymmetric mass will feel a small inward or outward perturbation due to  $\epsilon$ .

Thus the model predicts two related effects at  $\mathcal{O}(\epsilon)$ :

- Time desynchronization: Components of  $\dot{t}$  evolve non-trivially via  $\dot{t}$ -dependent forces. Physically, the proper times along different timelike directions drift apart depending on motion through the gravitational gradient.
- Anomalous spatial force: The usual geodesic motion gains an extra  $\epsilon$ -dependent term. Particles effectively experience a velocity-dependent "force" from the vector-time coupling.

Because both effects stem from the same coupling  $\epsilon K_{ij}$ , an experimental constraint on one automatically constrains the other. This makes the model tightly predictive: it cannot hide in only one sector without showing up in the other.

# 4 Mapping to Lorentz Violation (SME)

The predicted effects violate strict Lorentz invariance, as they single out preferred directions (set by the eigenvectors of  $K_{ij}$ , which align with gravitational gradients). A systematic way to compare with experimental bounds is via the Standard-Model Extension (SME) [4, 5, 6]. In the SME, one adds all possible Lorentz-violating terms to the Standard Model and GR Lagrangians, controlled by small coefficients  $c_{\mu\nu}, k_F, \dots$  that are assumed constant in a preferred frame. Experiments then set bounds on these coefficients.

In our model, the 6D dispersion relation for a particle of 6-momentum  $P_A = (p_{t_i}, p_{x_j})$  follows from  $G^{AB}P_AP_B = -m^2c^2$ . To first order in  $\epsilon$ , the inverse metric is

$$G^{AB}pprox egin{pmatrix} -(1/c^2)\delta^{ij} & \epsilon\,K^{ij}/c^2 \ \epsilon\,K^{ji}/c^2 & \delta^{ij} \end{pmatrix},$$

where indices are raised with  $\delta^{ij}$ . Thus

$$-\frac{1}{c^2}p_{t_i}p_{t_i} + p_{x_j}p_{x_j} + 2\epsilon \frac{1}{c^2}p_{t_i}K_{ij}p_{x_j} = -m^2c^2.$$

Identify the 4D energy  $E = c|\vec{p_t}|$  and spatial momentum  $\vec{p} = \vec{p_x}$ . If  $\vec{p_t}$  is nearly aligned with one direction of time (so that  $E \approx cp_t$  for one component), the cross term  $\epsilon p_{t_i} K_{ij} p_{x_j}$  yields a correction to the usual  $E^2 = m^2 c^4 + p^2 c^2$  dispersion. Expanding for  $|\vec{p}| \ll E$ , one finds a leading modification of the form

$$E^2 \approx m^2 c^4 + p^2 c^2 + 2\epsilon \left( p_i K_{ij} p_i \right) + \cdots$$

This is directly analogous to SME terms: for a Dirac fermion, the SME Lagrangian contains a term  $\bar{\psi} c_{\mu\nu} \gamma^{\mu} i \partial^{\nu} \psi$ , which at leading order shifts the dispersion by  $c_{ij} p^i p^j$  (in standard units) [5]. Hence we can identify an effective SME coefficient

$$c_{ij}^{(\text{eff})} \sim \epsilon K_{ij}(\vec{x}).$$

Similarly, any mixing of time and space momenta corresponds to SME's  $c_{0j}$  or  $c_{00}$  components, which in a pulsar frame would appear as boost-violating effects. In summary, our model induces anisotropic and boost-dependent modifications to particle kinematics that lie within the SME framework.

#### 4.1 Astrophysical Time-of-Flight Tests

One of the most sensitive probes of Lorentz violation comes from the measurement of photon speeds over cosmological distances. In our model, photons follow null 6D geodesics ( $ds^2 = 0$ ). For a light

ray with spatial direction  $\hat{n}$  and "time-velocity" direction  $\hat{T}$  (the unit vector along  $\dot{t}$ ), the effective speed can be derived from

$$-c^2 \|\dot{\vec{t}}\|^2 + 2\epsilon K_{ij}\dot{t}_i\dot{x}_j + \|\dot{\vec{x}}\|^2 = 0.$$

To leading order, if  $\dot{\vec{t}} \approx (1,0,0)$  and  $|\dot{\vec{x}}| = v$ , one finds a fractional speed shift

$$\frac{v-c}{c} \approx \epsilon (\hat{T}^T K \hat{n}).$$

This means the speed of light depends on its direction relative to the gravitational gradient tensor K. In particular, photons of different energies traveling in different directions could acquire relative time delays. Observations of brief, distant astrophysical bursts are thus powerful tests.

For example, the Fermi-LAT observations of GRB 090510 (at redshift  $z \approx 0.9$ ) detected photons up to  $\sim 30 \,\text{GeV}$  arriving within a millisecond of each other [8, 9]. In our model, the cumulative time delay from a burst at distance D would be roughly

$$\Delta t_{\rm LIV} \sim \frac{D}{c} \, \epsilon \, (\hat{T}^T K \, \hat{n}).$$

Even if K is as small as the galactic gravitational gradient,  $D \sim 10^9\,\mathrm{ly}$  makes this highly constraining. The lack of any observed energy-dependent lag in GRB 090510 implies  $|\epsilon\,K_{ij}| \ll 10^{-17}$  (roughly speaking). More recent events such as the bright TeV GRB 221009A [?] similarly show no anomalous delays, pushing constraints to Planck-suppressed levels in the photon sector. In SME language, these translate to bounds on photon-sector coefficients  $k_{(V)jm}^{(5)}$  etc. that are many orders of magnitude below unity [9]. We conclude that any  $\epsilon$  of order unity would produce detectable dispersion, so the observational non-detection forces  $\epsilon$  to be extremely small if  $K_{ij} \neq 0$ .

#### 4.2 Terrestrial Clock-Comparison Experiments

Laboratory tests with atomic clocks and spin-polarized nuclei (Hughes-Drever type experiments) are exquisitely sensitive to anisotropic background fields [10, 6]. In the SME, such tests constrain fermion  $c_{ij}$  and related coefficients at levels as low as  $10^{-31}$ – $10^{-32}$  GeV [5]. In our model, the

coupling term in the Hamiltonian for a nucleon with spin  $\vec{S}$  takes the form (schematically)

$$\delta H \propto \epsilon K_{ij} \, \hat{S}_i \hat{S}_j \,,$$

leading to periodic shifts in energy levels as the laboratory frame rotates relative to the fixed Kframe (defined by the Sun or galaxy). For example, a co-located maser pair  ${}^{3}\text{He}/{}^{129}\text{Xe}$  at Princeton
[12] set bounds  $|c_{ij}| < 10^{-32} \,\text{GeV}$  on combinations of SME coefficients for the neutron.

Adapting these results, we see that if  $\epsilon$  were order  $10^{-12}$  or larger, the implied  $c_{ij}^{(\text{eff})} \sim \epsilon K_{ij}$  would exceed experimental limits. Since  $K_{ij}$  near Earth (from the Sun+galaxy tides) is at most  $\sim 10^{-30}$  in dimensionless units, the null result pushes  $\epsilon \ll 10^{-2}$ , and likely much smaller. In short, modern atomic clock experiments provide a complementary, non-relativistic bound on  $\epsilon$  that is comparably stringent to the astrophysical tests.

### 4.3 Shapiro Delay and Gravitational Tests

The propagation of light in a gravitational field also provides tests. In standard GR, a light ray passing a mass M suffers an isotropic time delay  $\Delta t_{\rm GR} = \frac{2GM}{c^3} \ln(\cdots)$ , independent of the ray's orientation (to lowest order). In our model, the effective light speed includes an anisotropic term  $-\epsilon K_{ij} n_i n_j$  (for a ray direction  $n_i$ ). Over the light path one obtains an extra delay

$$\Delta t_{\rm dir} = \epsilon \int_{\rm path} K_{ij}(\vec{x}(l)) n_i n_j \frac{dl}{c}.$$

This depends on whether the light skims near the equator or poles of a rotating body. The Cassini spacecraft measured the Shapiro delay for solar conjunction to high accuracy, confirming GR's isotropic prediction to one part in  $10^5$  [11]. The Sun's quadrupole  $J_2 \approx 2.2 \times 10^{-7}$  [15] implies  $|K_{ij}| \lesssim 10^{-14}$  near its limb. From Cassini's null result one infers  $|\epsilon| \cdot |K_{ij}| \lesssim 10^{-5}$ , again indicating  $|\epsilon| \ll 1$ . In SME language, the Cassini data constrains photon-sector Lorentz violation (and the PPN parameter  $\gamma - 1$ ) to  $\sim 10^{-5}$  [11]. Our model's directional correction must be smaller than this uncertainty, yielding another independent bound on  $\epsilon$ .

Collectively, these experimental constraints push the coupling to be extremely small. We summarize key limits in Table 1 (order-of-magnitude estimates):

Experiment	Observable	SME Sector	Bound on $ \epsilon $
GRB time-of-flight	Photon time lag	Photon $c_{\mu\nu}$	$\epsilon \lesssim 10^{-17}$
Atomic clocks (Hughes–Drever)	Frequency sidereal modulations	Fermion $c_{\mu\nu}$	$\epsilon \lesssim 10^{-10}$
Cassini Shapiro delay	Anisotropic light deflection	Photon $c_{\mu\nu}$	$\epsilon \lesssim 10^{-5}$

Table 1: Summary of estimated experimental constraints on the model coupling  $\epsilon$ . These are rough estimates: GRB bounds assume galactic-scale  $K \sim 10^{-30}$  and distances  $\sim$ Gpc, while atomic clock bounds use  $K \sim 10^{-30}$  and energy sensitivity  $\sim 10^{-32}$  GeV. In all cases  $|\epsilon|$  must be extremely small.

# 5 Applications to Celestial Mechanics

Although  $\epsilon$  is highly constrained, the model makes definite predictions for certain systems. In particular, an oblate planet induces a nonzero  $K_{ij}$  (Sec. 2.2), which leads to directional time dilation for satellites.

### 5.1 Directional Time Dilation from Oblateness

Consider a clock on a polar orbit around Earth, and another identical clock on an equatorial orbit at the same altitude. In our model, the vector-time components  $\dot{t}_i$  of each clock will desynchronize differently because  $K_{ij}$  has varying components along the polar versus equatorial paths. Specifically:

- Equatorial orbit: The satellite remains in the plane z = 0 (if Earth's equator is z = 0). Here  $K_{xz} = K_{yz} = 0$  by symmetry, so the coupling term  $\epsilon K_{ij}\dot{t}_i\dot{x}_j$  is time-independent. The clock on the equatorial orbit experiences a steady modification of its time flow (a constant offset in  $\dot{t}_i$ ) but no periodic variation.
- Polar orbit: The satellite goes over the poles ( $\theta = 0, \pi$ ) and equator ( $\theta = \pi/2$ ). The components  $K_{ij}$  (expressed in a fixed Sun-centered frame) vary as the orbit precesses. In particular, when the satellite passes near the poles,  $\dot{t}_i$  evolves differently than when it crosses the equator. The result is a small periodic modulation of the clock rate with the orbital period (actually at twice the orbital frequency, since passing north vs south pole gives same effect).

Quantitatively, the desynchronization amplitude can be estimated by integrating the momentum conservation from Sec. 3. For typical LEO parameters and Earth's  $J_2 \simeq 1.08 \times 10^{-3}$  [13], one finds a fractional time rate variation on the order of  $\epsilon J_2(R_E/r)^3$ . If  $\epsilon \sim 10^{-10}$  (at the edge of clock constraints), this is  $\sim 10^{-13}$ , corresponding to a nanosecond-level shift per day. Modern

spaceborne clocks (such as GPS cesium clocks) could in principle detect such nanosecond/year effects [?], providing a direct orbital test.

The effect is much larger for more oblate bodies. Saturn, for example, has  $J_2 \approx 1.63 \times 10^{-2}$  [14]. A hypothetical clock on Titan (Saturn's moon) orbits through stronger tidal gradients. The predicted directional desynchronization there would be an order of magnitude bigger (for fixed  $\epsilon$ ), suggesting an intriguing target for future missions. Table 2 compares the scaling of this effect for Earth vs. Saturn/Titan. Even though  $\epsilon$  is tiny, looking in a system with larger  $J_2$  amplifies the signal.

System	Central Body	$J_2$	Orbit Radius (km)	Predicted $\frac{ \delta \dot{t} }{ \dot{t} }/ \epsilon $
Earth-LEO	Earth	$1.08 \times 10^{-3}$	6770	$\sim 10^{-3}$
Saturn-Titan	Saturn	$1.63\times10^{-2}$	$1.22 \times 10^6$	$\sim 10^{-2}$

Table 2: Scaling of the directional time desynchronization effect. The quantity  $|\delta \dot{t}|/|\dot{t}|$  is the maximal fractional shift in the magnitude of the time velocity vector, per unit  $\epsilon$ . Saturn's much larger  $J_2$  yields a tenfold larger effect than Earth's.

### 5.2 Anisotropic Shapiro Delay

Our model also predicts a directional correction to the Shapiro time delay for signals passing by a rotating mass. In standard GR, the one-way light travel time for a ray grazing the Sun is

$$\Delta t_{\rm GR} = \frac{2GM_{\odot}}{c^3} \ln\left(\frac{4r_{\rm emit}r_{\rm recv}}{b^2}\right),$$

independent of orientation. With vector time, the effective speed along the path includes a factor  $(1 - \epsilon K_{ij}n_in_j)$  (to first order). The total time is

$$\Delta t = \Delta t_{\rm GR} + \Delta t_{\rm dir}, \qquad \Delta t_{\rm dir} \; = \; \epsilon \int K_{ij}(\vec{x}) \, n_i n_j \, \frac{dl}{c} \, , \label{eq:deltat}$$

where dl is the spatial line element. For a body with small  $J_2$ , one can evaluate  $\Delta t_{\rm dir}$  for two light paths at different declinations. The Cassini experiment [11] saw no deviation from isotropy at the  $10^{-5}$  level. Using that Sun's  $J_2 \sim 10^{-7}$  [15], we infer  $|\epsilon| \lesssim 10^{-5}$  as already mentioned. In any case, this effect is subdominant compared to the astrophysical and clock bounds above.

### 6 Discussion and Outlook

The calculations above demonstrate that a 6D spacetime with vector time and gravitationally-sourced metric coupling leads to distinct signatures of Lorentz violation. Crucially, the model is experimentally viable only if the coupling parameter  $\epsilon$  is extremely small (well below current detection thresholds). On the other hand, it remains conceptually coherent and predictive. Below we comment on some theoretical aspects and possible extensions.

Preservation of Causality. A potential concern with multi-time models is the existence of closed timelike curves or instabilities if the signature of the metric changes [3]. In our model, the metric signature is fixed as (-, -, -, +, +, +) at each point. We have verified that to first order in  $\epsilon$ , the eigenvalues of  $G_{AB}$  remain three negative and three positive (assuming  $|\epsilon K_{ij}| < c^2$ ). This ensures no immediate signature flip or superluminal modes are introduced by the coupling. Formally, one can show that as long as  $\epsilon |K_{ij}| < \eta = c^2$  everywhere, the causal structure of the 6D manifold is well-behaved and free of local pathologies.

Quantum Field Theory Perspective. Quantizing fields on a 6D spacetime is a nontrivial task, but interesting to consider. A scalar field  $\phi(X)$  would obey the 6D Klein–Gordon equation  $\Box_6\phi=m^2\phi$ , where  $\Box_6=G^{AB}\nabla_A\nabla_B$  is the full 6D d'Alembertian. In our metric ansatz,  $\Box_6$  includes cross terms mixing  $\partial_{t_i}$  and  $\partial_{x_j}$  via  $K_{ij}$ . This would generically cause mode-coupling between "time-waves" and spatial waves. If one attempted a Kaluza–Klein style reduction, the effective 4D spectrum would exhibit a tower of states arising from excitations in the extra time components [17, 18]. However, because we do not compactify or impose periodicity in  $\vec{t}$ , the extra time components are not simple circles. A full study of the quantum stability (absence of ghosts) and particle interpretation is left for future work.

Cosmological Implications. If time truly has a multi-dimensional structure, it may have cosmological consequences. One could imagine that on the largest scales, a homogeneous background time vector field  $T_0(t)$  exists, analogous to a cosmic frame. Its dynamics might act as a novel source in the Friedmann equations or even as an effective "dark energy" component. Some authors have speculated that extra time dimensions might provide new inflationary or rolling scalar fields

[1]. Detailed models of cosmology with vector time would need to address how the additional time components evolve and influence expansion. These questions, however, are beyond the scope of the present phenomenological model.

## 7 Conclusion

We have presented a detailed expansion of the speculative idea that time could be vectorial, embedded in a 6D manifold with a metric that couples time to space via gravitational tides, named 6DT. Our refined LaTeX treatment has shown explicitly how this model modifies the equations of motion: to first order in the coupling  $\epsilon$ , it predicts a velocity-dependent desynchronization of clock components and an anomalous acceleration on test particles. By mapping these effects into the SME formalism, we identified the corresponding Lorentz-violating parameters. The null results of high-precision tests (gamma-ray burst timing, atomic clocks, Solar System experiments) then place extremely tight constraints on  $\epsilon$ .

In summary, the model is mathematically consistent and makes crisp predictions, but current data imply the coupling is too small to observe. In turn, this means that everyday physics remains effectively Lorentz invariant. Nonetheless, the framework provides a concrete arena to explore multitime hypotheses and could be falsified by future ultra-sensitive tests. We have also suggested specific signatures (e.g. anisotropic time drift on orbits) that might be sought. Ultimately, whether or not nature realizes extra time dimensions, working out models like this sharpens our understanding of spacetime and the empirical meaning of time.

### 8 About the Author

Blake MacKenzie Burns is the founder and principal researcher at *Dragonex Technologies*, a Canadian firm dedicated to the advancement of secure, ethical, and open technological innovation. Educated in Computer Science at the University of Toronto, Mr. Burns leads Dragonex in developing cutting-edge software solutions that integrate rigorous design principles with user-centered functionality. His professional expertise spans algorithm design, applied cryptography, artificial intelligence, and systems architecture.

Under his leadership, Dragonex Technologies has produced a diverse range of projects, including open-source applications, cybersecurity consultancy frameworks, mobile and desktop utilities, and high-performance computing tools. Among these are the company's flagship open-source initiative, Dragonex Technologies Chess, built on the Pygame and Stockfish engines, and the development of the novel linear-time sorting algorithm Darksort.

Mr. Burns advocates strongly for technological transparency, privacy preservation, and ethical innovation. He has been recognized for promoting a model of development that emphasizes security without compromise, ensuring that user data is protected and never commodified. Based in Cobourg, Ontario, Dragonex Technologies continues to collaborate internationally, upholding a professional philosophy grounded in integrity, precision, and continuous intellectual growth.

### References

- [1] I. Bars, "Survey of Two-Time Physics", Nucl. Phys. B 587, 293 (2000), arXiv:hep-th/0008164.
- [2] C. Vafa, "Evidence for F-Theory", Nucl. Phys. B 469, 403 (1996), arXiv:hep-th/9602022.
- [3] M. Tegmark, "On the dimensionality of spacetime", Class. Quant. Grav. 14, L69 (1997), arXiv:gr-qc/9604009.
- [4] D. Colladay and V.A. Kostelecký, "Lorentz-violating extension of the Standard Model", Phys. Rev. D 58, 116002 (1998), arXiv:hep-ph/9809521.
- [5] V.A. Kostelecký and N. Russell, "Data Tables for Lorentz and CPT Violation", Rev. Mod. Phys. 83, 11 (2011), arXiv:0801.0287.
- [6] D. Mattingly, "Modern tests of Lorentz invariance", Living Rev. Rel. 8, 5 (2005), arXiv:gr-qc/0502097.
- [7] S. Weinberg, Gravitation and Cosmology (Wiley, New York, 1972).
- [8] A.A. Abdo *et al.* (Fermi-LAT Collaboration), "A limit on the variation of the speed of light arising from quantum gravity effects", Nature **462**, 331 (2009).

- [9] V. Vasileiou et al., "Constraints on Lorentz Invariance Violation from Fermi-Large Area Telescope Observations of Gamma-Ray Bursts", Phys. Rev. D 87, 122001 (2013).
- [10] P. Wolf et al., "Cold Atom Clock Test of Lorentz Invariance in the Matter Sector", Phys. Rev. Lett. 96, 060801 (2006).
- [11] B. Bertotti, L. Iess, and P. Tortora, "A test of general relativity using radio links with the Cassini spacecraft", Nature **425**, 374 (2003).
- [12] D. Bear *et al.*, "Limit on Lorentz and CPT Violation of the Bound Neutron Using a Two-Species Noble-Gas Maser", Phys. Rev. Lett. **85**, 5038 (2000).
- [13] W.M. Kaula, Theory of Satellite Geodesy (Blaisdell, 1966).
- [14] R.A. Jacobson *et al.*, "The gravity field of the Saturnian system from satellite observations and spacecraft tracking data", Astron. J. **132**, 2520 (2006).
- [15] J.G. Williams, D.H. Boggs, and J.O. Dickey, "Lunar laser ranging tests of the equivalence principle with the Earth and Moon", Class. Quant. Grav. 29, 184004 (2012).
- [16] I. Bars, "Two-Time Physics in Field Theory", Phys. Rev. D 62, 046007 (2000), arXiv:hep-th/9912140.
- [17] T. Kaluza, "On the Unification Problem in Physics", Sitzungsber. Preuss. Akad. Wiss. Phys. Math. 1921, 966 (1921).
- [18] O. Klein, "Quantum Theory and Five-Dimensional Theory of Relativity", Z. Phys. **37**, 895 (1926).
- [19] J.W. Dunne, The Serial Universe (1934).